IEEE Access
Multidisciplinary | Rapid Review | Open Access Journal

Received 19 February 2024, accepted 19 March 2024, date of publication 27 March 2024, date of current version 12 April 2024.

Digital Object Identifier 10.1109/ACCESS.2024.3382581

RESEARCH ARTICLE

Multiple Antenna Configuration of LEO-MIMO Feeder Link for High Channel Capacity

DAISUKE GOTO, (Member, IEEE), KIYOHIKO ITOKAWA, KOYO TATEGAMI, AND FUMIHIRO YAMASHITA

NTT Access Network Service Systems Laboratories, NTT Corporation, Yokosuka 239-0847, Japan

Corresponding author: Daisuke Goto (daisuke.goto@ntt.com)

ABSTRACT We investigated low Earth orbit satellite (LEO) communications applying Multiple-Input/Multiple-Output (MIMO) technology to the feeder link transmission between a satellite and gateway antennas to improve the channel capacity. This paper calls LEO satellites using MIMO technology ''LEO-MIMO'' and considers satellite and gateway antenna configurations to improve the feeder link capacity. LEO-MIMO operates with a single LEO satellite equipped with multiple antenna elements and a gateway with multiple remotely located antennas. The conditions of the antenna configuration, such as the distances of satellite/gateway antenna elements and the number of antenna elements in the satellite and gateway, affect the channel capacity of LEO-MIMO. This paper reveals antenna configurations that improve the channel capacity for LEO-MIMO systems. Computer simulations show that the channel capacity of LEO-MIMO can achieve 4 bps/Hz at maximum higher than that of the conventional multi-beam system.

INDEX TERMS MIMO, LEO, number of antenna elements, GW antenna distance.

I. INTRODUCTION

NTT Labs. is studying space-integrated computing networks (NWs) for new infrastructures integrating multiple non-terrestrial network (NTN) systems such as high altitude platform stations (HAPS), low Earth orbit (LEO), and geo-stationary orbit (GEO) [1]. In these NWs, multilayered terrestrial networks (TNs)-NTN NWs are connected through optical and wireless communication and perform various data processes by distributed computing. They can also connect mobile terminals on the ground and make an ultrawide range of services possible.

One type of space-integrated computing networks is the LEO constellation system [1]. Fig. 1 shows an image of a typical LEO constellation system. The lower altitude enables wireless connectivity for small devices such as cellular phones. Since this system does not accommodate as many satellite-dedicated terminals as terrestrial mobile terminals, a higher system capacity is required.

Ways of increasing the system capacity are also being studied, such as wideband communications (more than 1GHz bandwidth in the Ka-band or Q/V-bands) [2], multilevel modulation (64, 128, and 256APSK) [3], and polarization multiplexing (V/H linear polarizations or right/left circular polarizations) [4]. However, the capacity improvement of these methods is limited due to restrictions on the available frequency bandwidth, transmission power, and polarization.

We focus on Multiple-Input Multiple-Output (MIMO) transmission technology applied to satellite communications [5], [6], [7], [8], [9]. MIMO technology can achieve a scalable channel capacity in proportion to the number

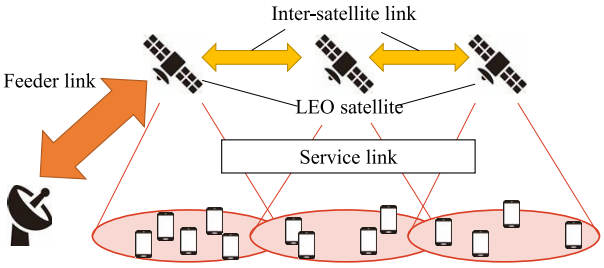

FIGURE 1. Mobile service by LEO constellation.

The associate editor coordinating the review of this manuscript and approving it for publication was Chan Hwang See.

© 2024 The Authors. This work is licensed under a Creative Commons Attribution-NonCommercial-NoDerivatives 4.0 License.
For more information, see https://creativecommons.org/licenses/by-nc-nd/4.0/

of transmitter (Tx) and receiver (Rx) antennas. In general, MIMO technology is considered to be useful in multipath-rich environments such as wireless LANs and cellular communication systems [10]. In these cases, the channels between Tx and Rx antennas tend to have a low correlation, so MIMO can achieve a high channel capacity. In contrast, since satellite communications are generally operated in line of sight (LOS) environments, the channel correlation becomes high, so MIMO technology cannot be applied directly.

To date, we have studied applying MIMO technology to LEO feeder links by using multiple antennas for satellites and gateways (GWs). Fig. 2 shows the overall LEO-MIMO configuration. The satellite is equipped with a phased array antenna and a GW with multiple large antennas. The phased array antenna forms multiple beams for multi-stream transmission to the multiple antennas of the GW to improve the channel capacity. Since the GW has large antennas for the satellite feeder links, effects on the multipath channel due to shielding and reflection are very small. In this case, the channel correlation is basically determined by the path lengths between Tx and Rx antennas and the wavelength of the center frequency. Therefore, antenna positioning for both the satellite and GW is very important to achieve high capacity with low correlation.

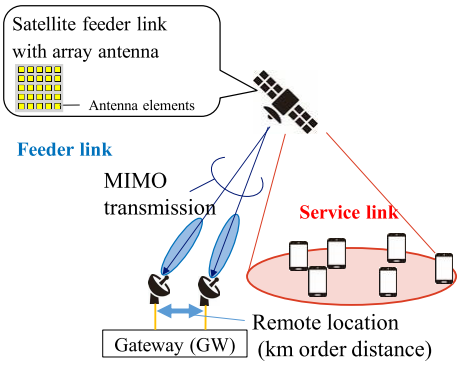

FIGURE 2. LEO-MIMO system with multiple antenna feeder links accommodating large number of mobile terminals in service link.

In the case of LEO satellite communications, the distance between the satellite and the GW is even larger than that of terrestrial communications. Therefore, GW antennas are remotely located to increase the arrival angles between GW antennas and achieve low correlation [11]. For satellite antennas, the antenna elements should be placed with a spacing of half a wavelength for grating lobe suppression, and the total antenna length cannot be large due to onboard space restriction. The previous studies considered capacity increase in LEO service links by applying Massive MIMO technology and capacity analysis of antenna spacing for GEO [11], [12], [13], [14]. However, there has been no study on stochastic channel capacity increase in LEO feeder links using phased arrays, depending on the number of Tx and Rx antennas and antenna spacing of them.

In this paper, we clarify the appropriate settings for the GW antennas' distance and the number of satellite phased array antenna elements to improve the MIMO channel capacity using computer simulation. For simplicity, we consider the use of two GW antennas. We confirm the effect of improving the MIMO channel capacity with the number of phased array elements in the LEO-MIMO feeder link.

This paper is organized as follows. In Section II, we provide a brief description of the LEO-MIMO feeder link system. In Section III, we explain the antenna configuration of the satellite and ground GW. In Section IV, we evaluate the channel capacity using computer simulation to clarify the effect of MIMO capacity improvement. Finally, we conclude the paper in Section V.

II. LEO-MIMO FEEDER LINK

This section describes the system model and the assumed channel model for the LEO-MIMO feeder link.

A. SYSTEM MODEL

Fig. 3 shows a downlink system model of the LEO-MIMO feeder link. The satellite has a phased array antenna system, and the GW has remotely located antennas that are aggregated to the GW through a wired connection. The satellite's phased array antenna forms multiple beams, of which the number is the same as those of MIMO multiplexes, and the direction of each beam is directed to each GW antenna. Data is converted in parallel for multiplexing, and each data sequence is modulated and converted to the RF frequency and then transmitted on each beam. In the baseband system, the signals received at the GW are expressed as follows when the number of satellite Tx antennas is N_t and the number of GW Rx antennas (same

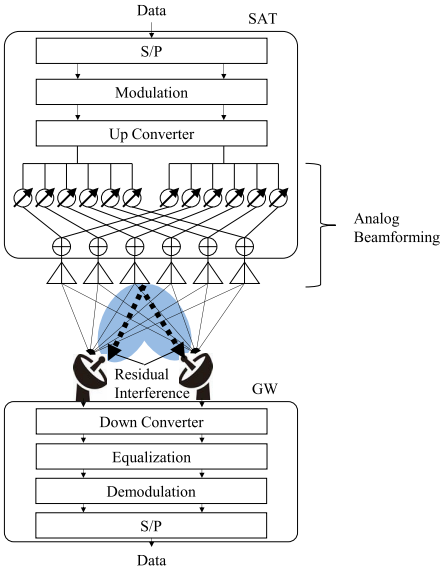

FIGURE 3. LEO-MIMO feeder link system model (downlink) with analog beamforming and receiver equalization.

as the number of satellite beams) is N_r:

$$\mathbf{r} = \mathbf{H}\mathbf{x} + \mathbf{n}$$
$$\begin{pmatrix} r_1 \\ \vdots \\ r_{N_r} \end{pmatrix} = \begin{pmatrix} h_{11} & \cdots & h_{1N_t} \\ \vdots & \ddots & \vdots \\ h_{N_r1} & \cdots & h_{N_rN_t} \end{pmatrix} \begin{pmatrix} x_1 \\ \vdots \\ x_{N_t} \end{pmatrix} + \begin{pmatrix} n_1 \\ \vdots \\ n_{N_r} \end{pmatrix} \tag{1}$$

where $\mathbf{r}$ is an N_r-dimensional received signal vector with the received signal component r_k in the k^{th} row, and $\mathbf{x}$ is an N_t -dimensional transmitted signal vector with the transmitted signal component x_k in the k^{th} row transmitted from the k^{th} transmitting antenna. The vector $\mathbf{n}$ denotes a noise vector of dimension N_r. The component n_k in the k^{th} line is the noise component at the k^{th} receiving antenna, which is independent identically distributed (i.i.d.) random noise with a zero-dispersion complex Gaussian distribution. The channel matrix $\mathbf{H}$ is an $N_r \times N_t$ matrix, where the k-by-l channel component h_{kl} denotes the complex channel component from the l^{th} transmitting antenna to the k^{th} receiving antenna. In this study, only direct waves are considered for channel conditions. This is because satellite feeder links are basically constructed in line-of-sight environments and the GW antenna is assumed to use a large reflector antenna, so the multipath components are negligible compared with direct waves. Considering the free space loss a_{kl} and the phase offset of the direct path, the channel component h_{kl} is expressed as follows;

$$h_{kl} = a_{kl} \times \exp\left(-\mathrm{j}\frac{2\pi}{\lambda} d_{kl}\right) \tag{2}$$

where

$$a_{kl} = \frac{\lambda}{4\pi d_{kl}} \tag{3}$$
$$\lambda = \frac{c_0}{f}. \tag{4}$$

Here, c_0 is the speed of light, and d_{kl} is the path length from the l^{th} Tx antenna to the k^{th} Rx antenna. The parameter λ expresses the wavelength of frequency f.

The vector $\mathbf{x}$ is obtained by multiplying the N_r-dimensional transmitting data vector $\mathbf{s}$ by the beamforming matrix $\mathbf{B}$ as follows:

$$\mathbf{x} = \mathbf{B}\mathbf{s}$$
$$\begin{pmatrix} x_1 \\ \vdots \\ x_{N_t} \end{pmatrix} = \begin{pmatrix} b_{11} & \cdots & b_{1N_r} \\ \vdots & \ddots & \vdots \\ b_{N_t1} & \cdots & b_{N_tN_r} \end{pmatrix} \begin{pmatrix} s_1 \\ \vdots \\ s_{N_r} \end{pmatrix}. \tag{5}$$

The beamforming matrix $\mathbf{B}$ is an $N_t \times N_r$ matrix, where the k-by-l channel component b_{kl} is the beamforming component for transmission from the l^{th} transmitting antenna to the k^{th} receiving antenna. In this paper, for simplicity, each beam is directed to the desired receiving antenna by in-phase combining, so b_{kl} is calculated as follows:

$$b_{kl} = \exp\left(\frac{\mathrm{j}2\pi}{\lambda}\Delta d_{kl}\right). \tag{6}$$

Here, Δd_{kl} is the path length difference between d_{kl} and d_{11} as follows:

$$\Delta d_{kl} = d_{kl} - d_{11}. \tag{7}$$

Each beam is formed without consideration of interference from other beams. Therefore, the equalization in the GW reduces the interference from undesired signals to obtain the desired signal vector $\tilde{s}$ by multiplying the received signals by the weight matrix $\mathbf{W}$ as follows:

$$\tilde{\mathbf{s}} = \mathbf{W}\mathbf{r}$$
$$\begin{pmatrix} \tilde{s}_1 \\ \vdots \\ \tilde{s}_{N_r} \end{pmatrix} = \begin{pmatrix} w_{11} & \cdots & w_{1N_r} \\ \vdots & \ddots & \vdots \\ w_{N_r1} & \cdots & w_{N_rN_r} \end{pmatrix} \begin{pmatrix} r_1 \\ \vdots \\ r_{N_r} \end{pmatrix}. \tag{8}$$

The component w_{lk} is the weight parameter to be multiplied to demodulate the l^{th} transmitted data for the k^{th} received signal. When using Minimum Mean Square Error (MMSE), the weight matrix $\mathbf{W}$ is calculated as follows:

$$\mathbf{W} = \widetilde{H_B}^H \left(\widetilde{H_B}\widetilde{H_B}^H + \mathbf{n}\mathbf{I}_{N_r}\right)^{-1}, \tag{9}$$

where

$$\mathbf{H_B} = \mathbf{HB}. \tag{10}$$

Here, $(\cdot)^H$ denotes the Hermitian transpose, and $\mathbf{I}_{Nr}$ denotes an $N_r \times N_r$ identity matrix. The matrix $\widetilde{H_B}$ means the channel estimation parameters of $\mathbf{HB}$.

III. ANTENNA CONFIGURATION STUDY TO IMPROVE CHANNEL CAPACITY

This section describes the antenna configuration of the satellite and GW for improving the channel capacity. Fig. 4 shows the concept behind our antenna configuration study. The multi-beam transmission shown in (a) is a conventional system in this paper. It achieves multiplex transmission with only multi-beams of satellites (without the operation of (8)) and may reduce inter-GW interference by increasing the number of satellite antenna elements and by increasing the distance between GW antennas sufficiently to increase beam isolation. In other words, system (a) must impose severe constraints on the number of satellite antenna elements and the distance of GW antennas to sufficiently reduced interference. In comparison, the proposed MIMO transmission system (b), which uses receiver interference cancellation, may improve the channel capacity compared with (a) in the case that inter-GW interference occurs, but the correlation of the MIMO channels becomes low. This also indicates that (b) may relax the constraints on the number of satellite antenna elements and the distance of GW antennas. This paper compares channel capacities in terms of the number of satellite antennas and GW antennas' distance.

Although the antenna gain, transmission power, and receiver G/T have to be taken into account for link budget calculation, this study determines the signal-to-noise power ratio (SNR) between the satellite and the GW antennas in advance

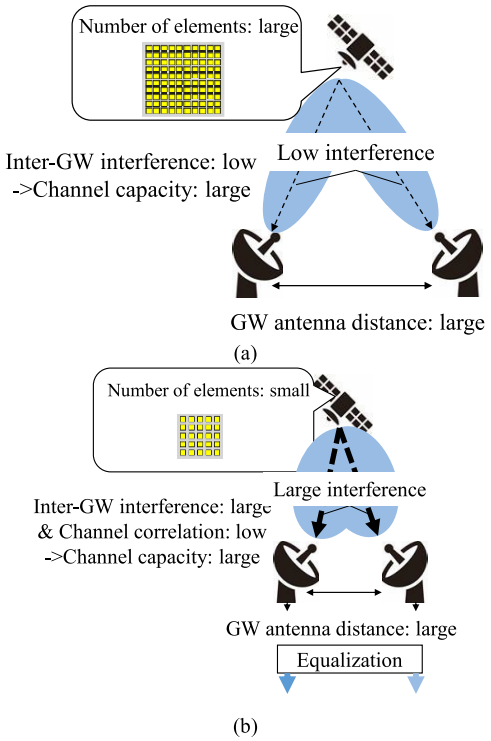

FIGURE 4. Capacity comparison between (a) conventional multi-beam system and (b) proposed LEO-MIMO system, in terms of antenna configuration.

to focus on the relationship between antenna configuration and channel capacity. The antenna pattern of each satellite array element is assumed to be isotropic.

On the other hand, the main beam of GW antennas is sharply directed in the satellite direction at all times by using a machine-tracking function.

IV. SIMULATION EVALUATION

This section describes the simulation details and evaluates the channel capacity by computer simulation.

A. SIMULATION DETAILS

We evaluated the channel capacity by computer simulation. Fig. 5 shows the simulation model. First, the satellite and the GW were placed in cartesian coordinates. Then, the channel matrix $\mathbf{H}$ was determined on the basis of (1) – (3). As described above, transmission power, receiver G/T, and antenna gain are not taken into account, but signal and noise power are determined from a preset SNR per the GW's receiving antenna. The channel capacity was calculated from the demodulated signals obtained from (5) - (10), in which MIMO calculates the weight matrix $\mathbf{W}$ with the ideal estimated $\mathbf{H}$. In contrast, the conventional system (a) does not use the weight matrix $\mathbf{W}$. The channel capacity C was calculated as follows:

$$C = \sum_{t=1}^{N_r} \log_2 (\gamma_t + 1) . \tag{11}$$

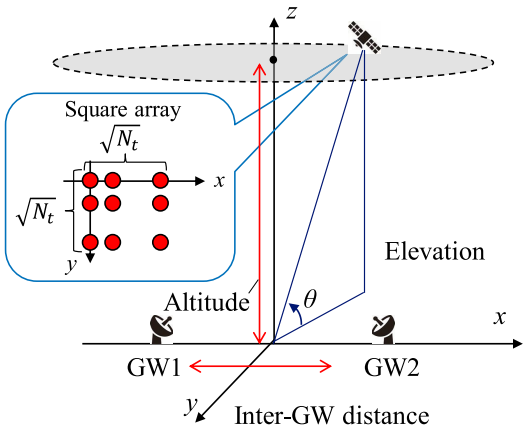

FIGURE 5. Feeder link simulation model, in which elevation of satellite is fixed, and satellite rotates in azimuthal direction relative to GW.

TABLE 1. Simulation parameters.

System Parameters	Parameter Values
Center frequency	20 GHz (Ka-band down link)
Channel model	Direct propagation
Interference mitigation	1. Multi-beam of in-phase combination (conventional) 2. MIMO (1.conventional w/ MMSE) (proposed)
Satellite (Transmitter)	
Altitude	500 km
Elevation	45°, 60°
Azimuth	0-359°
Antenna element pattern	Isotropic
Array antenna	Square array
Number of antennas per side of square array $\sqrt{N_t}$	10, 20, …, 100
Distance of array elements	7.5 mm (1/2 wavelength)
GW (Receiver)	
Received SNR	10 dB, 15 dB
Number of antennas N_r	2
Distance of antennas	10 km, 20 km, 30 km

The parameter γ_t indicates the signal-to-interference-plus-noise ratio (SINR) of the t^{th} component $\tilde{s}_t$ of the demodulated signal $\tilde{\mathbf{s}}$. In the feeder link simulation model, the elevation of the satellite was fixed, and the satellite rotated in the azimuthal direction relative to the GW. All the azimuth angles were swept, and the cumulative density function (CDF) was calculated. We evaluated CDF capacity values in terms of low (1%) and median (50%) values.

The configurations of the satellite phased array antenna and the GW antennas are shown in Fig. 5. The satellite antenna was a square array, of which the antenna elements spacing was set to be an equally spaced half of the wavelength. The number of antennas per side of the square array was $\sqrt{N_t}$. The number of GW antennas N_r was set, but in the case of SISO, only one GW antenna was used, that is, $N_r = 1$.

The simulation parameters are shown in Table 1. The frequency was set to 20 GHz, assuming a Ka-band downlink.

The elevation angle was fixed at 45° or 60°. When the satellite was located at high elevation angles from the GW, Tx and Rx antennas were located in the boresight direction, resulting in sharper beam directivity and low channel correlation. In this case, the channel capacity tends to be higher for multi-beam and MIMO satellites. On the other hand, lower elevation environments may degrade the channel capacity. In contrast, the capacity of SISO is assumed to be uniquely determined by the SNR. Since the simulation assumes that the SNR is constant at 10 dB or 15 dB, the capacity of SISO results in the same value. Therefore, the purpose was to clarify the conditions under which a sufficient channel capacity for MIMO can be obtained even in severe conditions.

B. SIMULATION RESUTLS

Fig. 6 shows a comparison of 1% and 50% values of the CDFs for the channel capacity versus the number of satellite antenna elements for the conventional multi-beam and the proposed MIMO satellites at 60° elevation. For reference, the SISO channel capacity with one GW is also shown to validate the advantages of multi-transmission techniques. You can see that the SISO performance remained at a constant capacity because of the fixed SNR in the simulation. In contrast, the two multi-transmission techniques showed improvements in capacity with an increase in the number of satellite antenna elements. These results were not due to an increase in the antenna gain because the SNR was constant regardless of the number of antennas in this simulation. Therefore, we can see that the results can be attributed to the improvement in SINR since the beam directivity of the phased array antennas became sharper and the MIMO channel correlation became lower as the number of antennas increased.

To demonstrate the advantages of multi-beam and MIMO satellite techniques, their capacity performances for both 1% and 50% values must be at least superior to those of the SISO satellite system. The results for the 1% values show that the characteristics of the two techniques improved with larger $\sqrt{N_t}$ and D, and they showed almost equivalent performances. The superiority to SISO was confirmed under the following conditions: $\sqrt{N_t} = 30$ or more for $D = 30$ km, $\sqrt{N_t} = 50$ or more for $D = 20$ km, and $\sqrt{N_t} = 90$ or more for $D = 10$ km. The 50% values show a difference in characteristics between the two techniques and the superiority of MIMO. Both techniques reached the approximate saturation point of approximately 7 [bps/Hz] at $\sqrt{N_t} = 40$ or more for $D = 30$ km, $\sqrt{N_t} = 50$ or more for $D = 20$ km, and $\sqrt{N_t} = 100$ for $D = 10$ km, but the MIMO performances were superior to multi-beam in other points.

Fig. 7 shows the capacity when the elevation angle was set to 45°. The results show that MIMO had advantages over

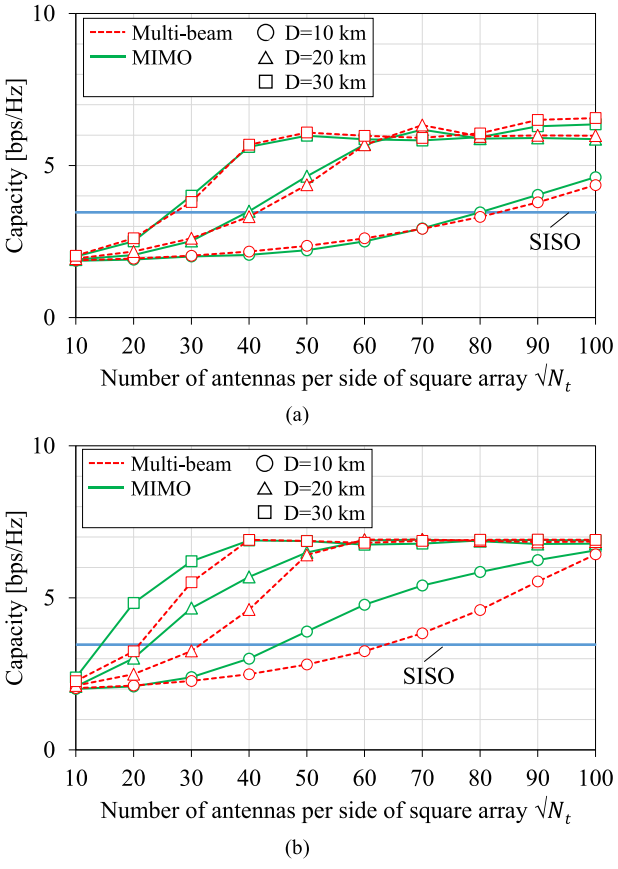

FIGURE 6. Channel capacity of CDF (a) 1% and (b) 50% values versus number of array antenna elements with 60° elevation at SNR = 10 dB.

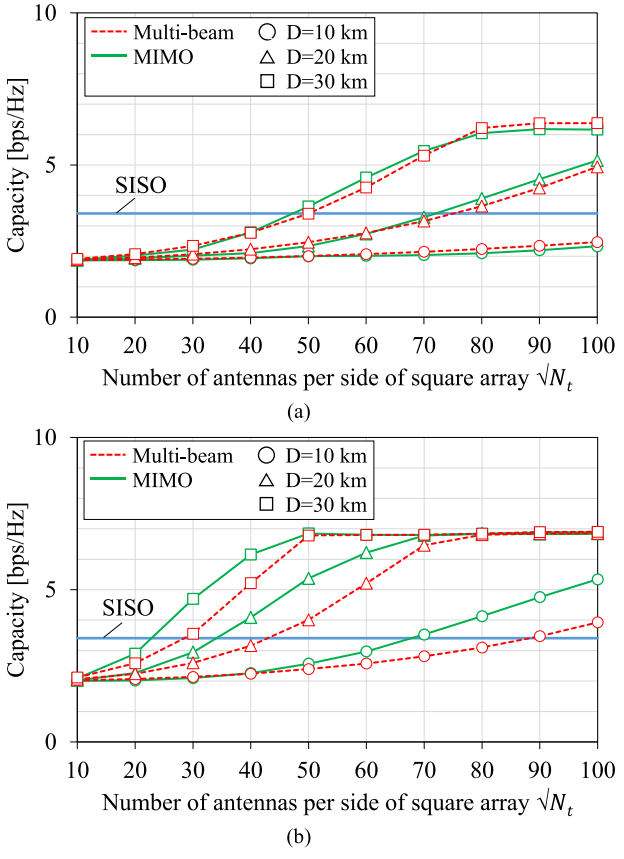

FIGURE 7. Channel capacity of CDF (a) 1% and (b) 50% values versus number of array antenna elements with 45° elevation at SNR = 10 dB.

multi-beam systems for both 1% and 50% values until the saturation points were reached, the same as for 60° elevation. However, the MIMO capacity improvement was smaller than that for 60° elevation, but this is due to the fact that a low elevation angle cannot achieve sufficient beam isolation. Note that at 45° elevation, the results for the 1% value of $D = 10$ km were inferior to the capacity of SISO for the entire region for both systems, indicating that it is difficult to obtain sufficient capacity with MIMO with any antenna configuration.

Fig. 8 shows the capacity comparison when SNR = 15 dB at an elevation angle of 60°. Unlike SNR = 10 dB, the results show a difference between the two techniques, especially for the 1% value, for which the superiority of MIMO for the entire region was confirmed. In particular, the maximum advantage of 2 bps/Hz was obtained at $\sqrt{N_t} = 30$ for $D = 30$ km, $\sqrt{N_t} = 50$ for $D = 20$ km, and $\sqrt{N_t} = 100$ for $D = 10$ km. A superiority of up to 3 bps/Hz was confirmed at $\sqrt{N_t} = 70$ for $D = 30$ km, $D = 20$ km, and $D = 10$ km, respectively. This indicates that the higher the SNR, the better the capacity performance for LEO-MIMO.

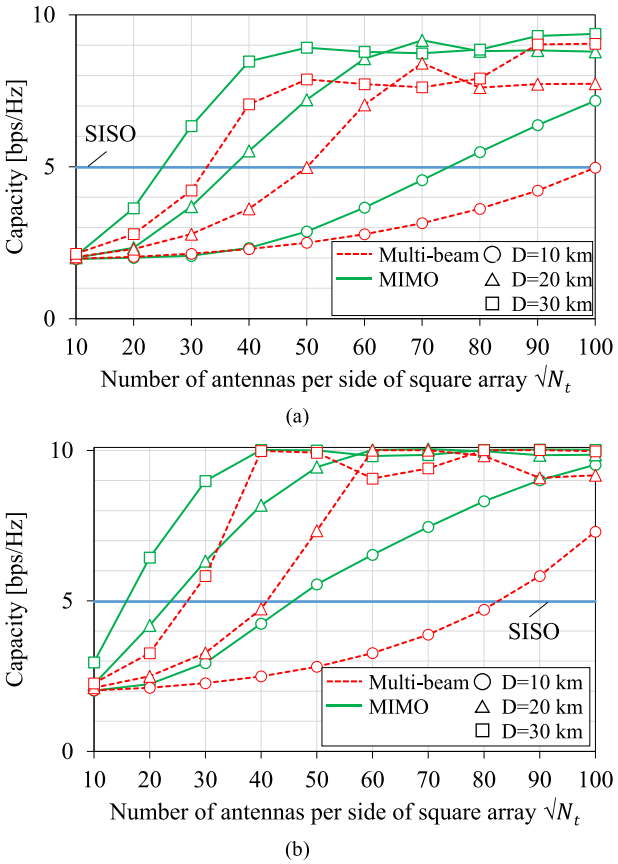

FIGURE 8. Channel capacity of CDF (a) 1% and (b) 50% values versus number of array antenna elements with 60° elevation at SNR = 15 dB.

Fig. 9 shows the evaluation of the 45° elevation at SNR=15 dB. Although the capacity performance degraded compared with 60° elevation, MIMO had superiority to the multi-beam system here as well, both for the 1% and 50%

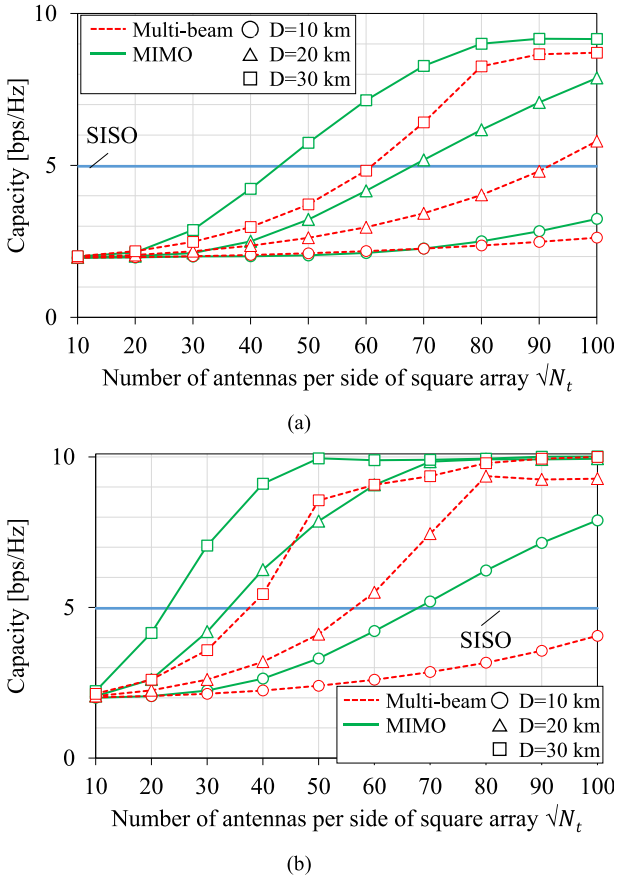

FIGURE 9. Channel capacity of CDF (a) 1% and (b) 50% values versus number of array antenna elements with 45° elevation at SNR = 15 dB.

values. In particular, the 50% value at $D = 10$ km showed a significant advantage, in which the MIMO improved over SISO at $\sqrt{N_t} = 70$ and above, while the multi-beam system showed a degradation in characteristics compared with SISO in all cases. Moreover, there was an improvement of approximately 4 bps/Hz at $\sqrt{N_t} = 100$ compared with the multi-beam system.

Finally, we summarize the conditions under which MIMO can achieve better capacity than the SISO and multi-beam systems even at the 1% value. When the number of satellite array antenna elements and the GW antenna distance must be minimized as much as possible to take space restrictions into account, the MIMO system can achieve high capacity by setting $\sqrt{N_t} = 60$ (3600 square array elements) and $D = 20$ km under the condition that SNR=15 dB can be achieved at a 45° elevation angle as the lowest elevation.

V. CONCLUSION

Our study focuses on the application of MIMO transmission technology to low Earth orbit satellites for feeder links. We examined the effect of improving the channel capacity on the basis of the number of satellite array antennas and the GW antenna distance. The MIMO technique can achieve a higher capacity than that of the conventional multi-beam

technique with a maximum advantage of 4 bps/Hz. Moreover, MIMO can improve capacity even for 1% CDF values at low elevation angles of 45° when the number of square array elements is set to 3600 and D = 20 km at SNR = 15 dB.

REFERENCES

[1] (2021). *NTT Press Release*. [Online]. Available: https://group.ntt/en/newsrelease/2021/05/20/210520a.html
[2] T. Rossi, M. De Sanctis, F. Maggio, M. Ruggieri, G. Codispoti, and G. Parca, "Q/V-band satellite communication experiments on channel estimation with alphasat Aldo Paraboni P/L," in *Proc. IEEE Aerosp. Conf.*, Big Sky, MT, USA, Mar. 2015, pp. 1–11.
[3] A. B. Ali Bachir, M. Zhour, and M. Ahmed, "Modeling and design of a DVB-S2X system," in *Proc. 5th Int. Conf. Optim. Appl. (ICOA)*, Kenitra, Morocco, Apr. 2019, pp. 1–5.
[4] P. Naseri, S. A. Matos, J. R. Costa, C. A. Fernandes, and N. J. G. Fonseca, "Dual-band dual-linear-to-circular polarization converter in transmission mode application to *K*/*Ka*-band satellite communications," *IEEE Trans. Antennas Propag.*, vol. 66, no. 12, pp. 7128–7137, Dec. 2018.
[5] C. Kato, M. Nakadai, D. Goto, H. Shibayama, and F. Yamashita, "Channel capacity analysis of satellite MIMO system depending on the orbital altitude," in *Proc. Adv. Commun. Satell. Syst. 37th Int. Commun. Satell. Syst. Conf. (ICSSC)*, Oct. 2019, pp. 1–16.
[6] R. T. Schwarz, A. Knopp, D. Ogermann, C. A. Hofmann, and B. Lankl, "Optimum-capacity MIMO satellite link for fixed and mobile services," in *Proc. Int. ITG Workshop Smart Antennas*, Feb. 2008, pp. 209–216.
[7] R. T. Schwarz, A. Knopp, B. Lankl, D. Ogermann, and C. A. Hofmann, "Optimum-capacity MIMO satellite broadcast system: Conceptual design for LOS channels," in *Proc. 4th Adv. Satell. Mobile Syst.*, Bologna, Italy, Aug. 2008, pp. 60–65.
[8] F. Yamashita, K. Kobayashi, M. Ueba, and M. Umehira, "Broadband multiple satellite MIMO system," in *Proc. VTC–Fall IEEE 62nd Veh. Technol. Conf.*, vol. 4, Sep. 2005, pp. 2632–2636.
[9] C.-I. Oh, S.-H. Choi, D.-I. Chang, and D.-G. Oh, "Analysis of the rain fading channel and the system applying MIMO," in *Proc. Int. Symp. Commun. Inf. Technol.*, Oct. 2006, pp. 507–510.
[10] K. P. Liolis, A. D. Panagopoulos, and P. G. Cottis, "Multi-satellite MIMO communications at Ku-band and above: Investigations on spatial multiplexing for capacity improvement and selection diversity for interference mitigation," *EURASIP J. Wireless Commun. Netw.*, vol. 2007, no. 1, pp. 30–41, Dec. 2007.
[11] R. T. Schwarz, A. Knopp, and B. Lankl, "The channel capacity of MIMO satellite links in a fading environment: A probabilistic analysis," in *Proc. Int. Workshop Satell. Space Commun.*, Sep. 2009, pp. 78–82.
[12] L. You, K.-X. Li, J. Wang, X. Gao, X.-G. Xia, and B. Ottersten, "Massive MIMO transmission for LEO satellite communications," *IEEE J. Sel. Areas Commun.*, vol. 38, no. 8, pp. 1851–1865, Aug. 2020.
[13] K.-X. Li, L. You, J. Wang, X. Gao, C. G. Tsinos, S. Chatzinotas, and B. Ottersten, "Downlink transmit design for massive MIMO LEO satellite communications," *IEEE Trans. Commun.*, vol. 70, no. 2, pp. 1014–1028, Feb. 2022.
[14] R. T. Schwarz, T. Delamotte, K.-U. Storek, and A. Knopp, "MIMO applications for multibeam satellites," *IEEE Trans. Broadcast.*, vol. 65, no. 4, pp. 664–681, Dec. 2019.

DAISUKE GOTO (Member, IEEE) received the B.E. degree in system engineering from Shizuoka University, in 2010, and the M.E. and Ph.D. degrees in electrical engineering and computer science from Nagoya University, Japan, in 2012 and 2020, respectively. In 2012, he joined the NTT Access Network Service Systems Laboratories, Japan. His current research interest includes satellite communication techniques.

KIYOHIKO ITOKAWA received the B.E. and M.E. degrees in electrical and electronic engineering from the University of Tsukuba, Japan, in 1998 and 2000, respectively. He is currently a Senior Research Engineer with the NTT Access Network Service Systems Laboratories. He joined the NTT Access Network Service Systems Laboratories, in 2000, and has been involved in developing wireless access systems, such as 802.11a wireless LAN systems and 26-GHz-band subscriber fixed wireless access systems. His current research interests include the research and development of satellite MIMO and IoT systems using LEO satellites.

KOYO TATEGAMI received the B.E. and M.E. degrees from the University of Fukui, in 2019 and 2021, respectively. In 2021, he joined the NTT Access Network Service Systems Laboratories, Japan. His current research interest includes satellite communication techniques.

FUMIHIRO YAMASHITA received the B.E., M.E., and Ph.D. degrees from Kyoto University, in 1996, 1998, and 2006, respectively. He is currently a Senior Research Engineer and a Supervisor with the NTT Access Network Service Systems Laboratories. He worked on modulation and demodulation schemes for broadband mobile satellite communications systems. He has been a part-time Lecturer with Kanto Gakuin University and the Muroran Institute of Technology, since 2018. His current interests include the research and development of disaster-relief and remote island satellite communications systems and satellite MIMO and IoT systems using LEO satellites.